Magnetization reversal and coercive force in ultrathin films with perpendicular surface anisotropy: Micromagnetic theory

Xiao Hu*
National Institute of Standards and Technology, Boulder, Colorado 80303
(Received 25 January 1996; revised manuscript received 6 December 1996)

Quasistatic magnetization reversal in ultrathin magnetic films with perpendicular surface anisotropy is discussed. In order to focus on the role of the surface anisotropy, magnetization is presumed uniform across the film plane, and its variation along the film normal is subject to micromagnetic analysis of a functional including the shape anisotropy energy from dipolar interactions. Different reversal processes—such as nucleations, coherent and incoherent rotations, domain-wall motion, and abrupt jumps—are found in films, depending on the values of shape anisotropy, surface anisotropy, exchange stiffness, and film thickness. The coercivity of ultrathin magnetic films in fields perpendicular to the film plane decreases with the square of the reciprocal of the film thickness, which coincides very well with experimental observations. Magnetization reversal processes resulting from applying in-plane external fields are also described.
[S0163-1829(97)07013-6]

I. INTRODUCTION

The mechanism of magnetization reversal in ultrathin films is discussed in this paper. Ultrathin magnetic films are of current interest for both academic study of magnetism and research for new technologies. Giant magnetoresistance (GMR) has been observed in Fe/Cr and other magnetic/nonmagnetic multilayer systems.[1] The square hysteresis loops and giant magneto-optical (MO) effects observed in Co/Au multilayers make them good candidates for MO storage media.[2] The nature of magnetization reversal in these materials plays a key role in determining their properties. To obtain a GMR, an in-plane external field switches a high-resistance antiparallel magnetization configuration between the magnetic layers into a low-resistance parallel magnetization configuration. In MO recording, a field perpendicular to the film plane is applied to reverse the magnetization in bit area.

The theoretical understanding of magnetization reversal has been the subject of much study, particularly as it relates to the magnetism of fine magnetic particles. It began with the Stoner-Wohlfarth model[3] in the late 1940's and continued with the development of the micromagnetic theory by Brown[4] in the late 1950's. Aharoni used a one-dimensional micromagnetic model which is applicable to thin films and multilayers to explain the reduction of coercive force by imperfections.[5]

In ultrathin magnetic films typically of 1 to 5 nm, the strong normal surface anisotropy greatly affects their stable magnetization states[6–13] and complicates their magnetization reversals.[8,14–17] Theoretically, spin reorientation undergoes two continuous phase transitions as the film thickness increases:[10–12] The stable state of magnetization changes from a uniform configuration normal to the film plane, to a canting configuration, and then to a uniform configuration parallel to the film plane if $K_s < \sqrt{AK_v}$, where K_s, K_v, and A are the surface anisotropy, volume anisotropy, and exchange stiffness.[10,12] The two phase boundaries for the above phases are given analytically as $a_{c1} = \sqrt{A/K_v}\ \tan^{-1}(K_s/\sqrt{AK_v})$ and $a_{c2} = \sqrt{A/K_v}\ \tanh^{-1}(K_s/\sqrt{AK_v})$, where a is equal to one half of the film thickness.[12] These phase transitions have been observed experimentally.[9] The effective volume anisotropy is $K_v^{\rm eff} = K_v - K_s/a$ (Refs. 8 and 12) for $a \geqslant a_{c2}$. In systems where $K_s \geqslant \sqrt{AK_v}$, there is a change from normal to canting, but the canting structure remains stable even at large thicknesses, which reduces the effect of large surface anisotropy. In this case the effective volume anisotropy should behave asymptotically as $K_v^{\rm eff} = K_v - E_s/a$, with $E_s = 2\sqrt{AK_v} - AK_v/K_s$.[12]

Since spin reorientations occur in very thin magnetic films of only several atomic layers, it is important to address the problem of whether the continuum approach is valid for these systems. For this purpose, Hu, Tao, and Kawazoe have studied a discrete model which includes the exchange coupling between neighboring atomic layers.[13] We found that adopting two scaling variables, $\hat{a}(N-2)\sqrt{K_v/A}$ and $K_s/\sqrt{AK_v}$, where $\hat{a}$ is the lattice spacing and N is the number of atomic layers, makes the results of the discrete and continuum models coincide. The continuum approach is thus justified in the study of ultrathin magnetic films of several atomic layers, and is adopted in the present study.

Because the normal anisotropy is confined to the surface of ultrathin magnetic films,[18,19] they are good samples for the study of surface effects on bulk properties. In a simple treatment for surface effects, one considers a surface quantity Q_s as a modification to the bulk quantity Q_v: $Q_v^{\rm eff} = Q_v + Q_s/L$, where L is the system size in the relevant direction. The system is thus governed by a uniform bulk-specified quantity $Q_v^{\rm eff}$. For ultrathin magnetic films with normal surface anisotropy, one has $K_v^{\rm eff} = K_v - K_s/a$,[8] and a single, first-order transition from the normal to the in-plane magnetization configuration is derived at a critical thickness $a_c = K_s/K_v$. This phenomenological argument is sufficient for systems with large exchange stiffness or small surface anisotropy such that $K_s/\sqrt{AK_v} \ll 1$, for which $a_{c1} \simeq a_{c2} \simeq a_c$. For systems with larger surface anisotropy, the canting structure exists over a wider range of film thickness, and the phenomenological argument no longer applies. This simple phenomenological consideration is an even poorer approximation when a perpendicular external field is applied to reverse the magnetiza-

tion in the film. According to the phenomenological argument, the coercivity should depend linearly on the reciprocal of the thickness: $H_{\perp c}=2(K_s/a-K_v)/M_s$, for $a<a_c$. However, experimentally the coercivity of ultrathin magnetic films in fields perpendicular to the film plane decreases with the reciprocal of the thickness raised to a power close to 2,[8,14–16] contrary to the above prediction.

A theory has been proposed to explain this observed exponent. This approach presumes uniform magnetization along the film normal and attributes the magnetization reversal in the sample solely to domain-wall motion in in-plane directions.[14,15] The coercivity, which is treated as equal to the propagation field of domain walls, is predicted to decay with the reciprocal of the thickness with an exponent of 5/2. There remains a discrepancy between this predicted exponent and the experimental value. Moreover, in certain samples of thin magnetic film, when the external field is applied, nucleation of magnetization reversal takes place, followed by wall motion.[17] In magnetic cylinders with diameters of 0.5 through 2 μm and thicknesses less than 2 nm, the magnetization is reversed as a whole by the external field.[20] Therefore, it is very important to investigate reversal processes by other than domain-wall motion in in-plane directions.

Since the existence of normal surface anisotropy is the most important feature of ultrathin magnetic films sandwiched by nonmagnetic layers,[21] we believe that a theory for magnetic phenomena in ultrathin magnetic films will be more intuitive if the nonuniformity of magnetic anisotropy in the direction of the film normal can be treated in a direct way. In the present work, we investigate nucleation of magnetic structures nonuniform in the direction of film normal as another possibility for the magnetization reversal in thin magnetic films, presuming that the magnetization configuration is uniform across the film plane. As far as magnetization is uniform in the directions within the film plane of infinite extension, varying or not varying in the normal direction, the demagnetization field is given by $4\pi M_s(z)$, as discussed by Mills,[22] and the contribution to the total energy can be summarized as $2\pi M^2 \sin^2\varphi(z)$. Although these expressions take a ''localized'' form, which simplifies the otherwise intractable analytic calculation, they include effects of all long-range dipole-dipole interactions. The above expressions have been used frequently in study of ultrathin magnetic films and they apply even in the presence of external field. Actually, Thiaville and Fert used an energy functional including the ''localized'' dipolar-interaction energy to study the coercive field.[10] What is lacking in their paper and what are the main results of the present work, are the detailed magnetization processes under different fields, and the explicit estimate of the thickness dependence of the coercive field.

The remainder of this paper is organized as follows. In Sec. II, analytical equations for the magnetization configuration under perpendicular external field are derived using a micromagnetic energy functional. In Sec. III, detailed reversal processes in ultrathin magnetic films are presented. The coercivity is evaluated and its dependences on the surface anisotropy and film thickness are clarified. Section IV is devoted to magnetic films subject to in-plane external fields. Discussions and summary are given in Sec. V.

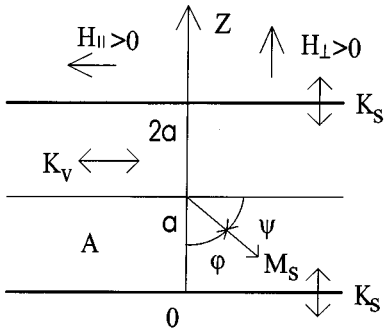

FIG. 1. Geometry of the system and notation used in this study.

II. CONFIGURATION OF MAGNETIZATION IN PERPENDICULAR FIELD

We start with the following functional for half of the total magnetic energy per unit area in a thin magnetic film with thickness $2a$ under a perpendicular field:[22,10,12]

$$\gamma=\int_0^a\left[A\left(\frac{d\varphi}{dz}\right)^2-K_v\sin^2\varphi+H_\perp M_s\cos\varphi\right]dz+K_s\sin^2\varphi(0), \tag{1}$$

where notations are shown in Fig. 1. The first term is the exchange-coupling term, the second term represents the volume anisotropy energy due to an intrinsic contribution $K_v^{\rm int}$ and the contribution from dipole-dipole interactions $K_v \equiv 2\pi M_s^2-K_v^{\rm int}$, the third term is the Zeeman energy term, and the last term is the vertical surface anisotropy term. The film thickness $2a$ is related to the number of atomic layers N by $2a=(N-2)\hat{a}$, where $\hat{a}$ is the lattice constant.[13]

The stable magnetization configuration is found by applying the variational technique to the energy functional (1). The Euler equation thus obtained can be reduced to the nonlinear equation concerning φ_a, the direction of magnetization at the film center.[12,23] For the configuration satisfying the condition $d\varphi/dz>0$ in $0\leqslant z\leqslant a$, this equation is given as

$$\frac{K_s}{\sqrt{AK_v}}=\frac{1+{\rm cn}^2[x_1,k_1]\tan^2(\varphi_a/2)}{1-{\rm cn}^2[x_1,k_1]\tan^2(\varphi_a/2)}\sqrt{\cos\varphi_a+h_\perp/2}\times\frac{{\rm sn}[x_1,k_1]{\rm dn}[x_1,k_1]}{{\rm cn}[x_1,k_1]}, \tag{2}$$

where

$$x_1=a\sqrt{K_v/A}\sqrt{\cos\varphi_a+h_\perp/2},$$

$$k_1=\sin\left(\frac{\varphi_a}{2}\right)\sqrt{(-1+\cos\varphi_a+h_\perp)/(2\cos\varphi_a+h_\perp)},$$

$$h_\perp\equiv H_\perp M_s/K_v, \tag{3}$$

if $-1+\cos\varphi_a+h_\perp>0$. Here ${\rm sn}[x,k]$, ${\rm cn}[x,k]$, and ${\rm dn}[x,k]$ are Jacobi elliptic functions. Using φ_a determined by the above equation, the total magnetization configuration in $0\leqslant z\leqslant a$ is expressed explicitly by

$$\tan\left(\frac{\varphi(z)}{2}\right)=\tan\left(\frac{\varphi_a}{2}\right)\mathrm{cn}[(a-z)\sqrt{K_v/A}\sqrt{\cos\varphi_a+h_\perp/2},k_1]. \tag{4}$$

For $-1+\cos\varphi_a+h_\perp<0$, the equation for φ_a is

$$\frac{K_s}{\sqrt{AK_v}}=\frac{\mathrm{dn}^2[x_2,k_2]+\mathrm{cn}^2[x_2,k_2]\tan^2(\varphi_a/2)}{\mathrm{dn}^2[x_2,k_2]-\mathrm{cn}^2[x_2,k_2]\tan^2(\varphi_a/2)}\frac{2\cos\varphi_a+h_\perp}{\sqrt{(1+\cos\varphi_a)(1+\cos\varphi_a+h_\perp)}}\frac{\mathrm{sn}[x_2,k_2]}{\mathrm{cn}[x_2,k_2]\mathrm{dn}[x_2,k_2]}, \tag{5}$$

with

$$x_2=a\sqrt{K_v/A}\sqrt{(1+\cos\varphi_a)(1+\cos\varphi_a+h_\perp)}/2,$$

$$k_2=\tan\left(\frac{\varphi_a}{2}\right)\sqrt{(1-\cos\varphi_a-h_\perp)/(1+\cos\varphi_a+h_\perp)}, \tag{6}$$

and the magnetic configuration in $0\leqslant z\leqslant a$ is given by

$$\tan\left(\frac{\varphi(z)}{2}\right)=\tan\left(\frac{\varphi_a}{2}\right)\frac{\mathrm{cn}[(a-z)\sqrt{K_v/A}\sqrt{(1+\cos\varphi_a)(1+\cos\varphi_a+h_\perp)}/2,k_2]}{\mathrm{dn}[(a-z)\sqrt{K_v/A}\sqrt{(1+\cos\varphi_a)(1+\cos\varphi_a+h_\perp)}/2,k_2]}. \tag{7}$$

The magnetization configuration for $a\leqslant z\leqslant 2a$ is easily obtained from symmetry. After determining the nonuniform magnetization configuration by Eqs. (2)–(7), one should estimate the magnetic energy associated with the structure and then compare it with the energy of the trivial configuration $\varphi=0$, in order to tell which state is metastable. A simpler way of accomplishing this is available: since at $H_\perp=0$ the configuration $\varphi=0$ is stable, it will remain metastable for small positive fields, while the configuration determined by Eqs. (2)–(7) is unstable in these fields. As the external field increases, the difference between the energies associated with these two states decreases, and disappears at some field. This field strength is defined as the nucleation field, above which a nonuniform magnetic structure is nucleated and is metastable. By setting $\varphi_a=0$ in Eqs. (2) and (3), one obtains the equation for the nucleation field $h_{\perp n}$ (Ref. 10)

$$\frac{K_s}{\sqrt{AK_v}}=\sqrt{1+h_{\perp n}/2}\,\tan(a\sqrt{K_v/A}\sqrt{1+h_{\perp n}/2}). \tag{8}$$

A positive nucleation field determined by the above equation, can be shown analytically to be smaller than $2(K_s/a-K_v)/M_s$, which happens to be equal to the coercive force derived by the phenomenological argument, by noting that $x<\tan x$ for $0<x<\pi/2$. This relation guarantees that the change in the magnetization configuration occurs at a field smaller than the coercive force predicted by the phenomenological theory, which assumes uniform reversal *a priori* and predicts an abrupt jump in direction of magnetization at the coercive force. As the external field is increased beyond a certain value, Eqs. (2) and (5) no longer have solutions. Magnetization reversal should occur at this field, and the system attains the new stable state $\varphi=\pi$. The value of the field at which this reversal occurs is defined as the coercive force in the present approach.

For systems possessing canting magnetization configurations at zero field, the nucleation field determined by Eq. (8) is negative. In such a system, there exists a saturation field $H_{\perp s}$, with the same absolute value of the nucleation field, at which the magnetic configuration saturates to uniform normal configuration.

In the first equations of (3) and (6), one finds that the film thickness a is multiplied by the square root of the strength of the external field. This relation between the film thickness and the external field is characteristic only of magnetic structures nonuniform in the direction of film normal. It implies a decrease of coercivity with the square of the reciprocal of the thickness as observed experimentally, provided that the other contributions from the external field in Eqs. (2), (3), (5), and (6) are small or cancel each other. This feature of the coercivity will be discussed later with numerical results.

Equations (2)–(7) describe magnetic states in systems possessing downward magnetizations when the field decreases to zero. With the symmetry of the magnetic properties of the system, we can derive easily the hysteresis phenomenon of the system from the above equations. We note that Eq. (8) can also be taken as an expression of the critical thickness a_{c1} at which the spin-reorientation transition from uniform, vertical configuration to canting occurs under an external field $h_\perp$.

III. REVERSAL PROCESSES AND COERCIVITY

The phase diagram for responses of thin films to perpendicular external fields derived from the above equations is shown in Fig. 2. For zero field, there are three phases, the uniform normal (I), canting (II), and uniform in-plane (III) phases, which are separated by the solid phase boundaries in Fig. 2.[10,12,13] Subphases in which the system responds to the external field in different ways are observed. In the Ia phase, the system remains in a downward uniform configuration (DUC) under small field and then jumps abruptly to a reversed upward uniform configuration (UUC) as the field increases to the coercivity $H_{\perp c}$. The hysteresis loop in this subphase is exactly rectangular. Since it is equal to the nucleation field in this phase, the coercive force is determined by Eq. (9) and is smaller than the coercive force evaluated by

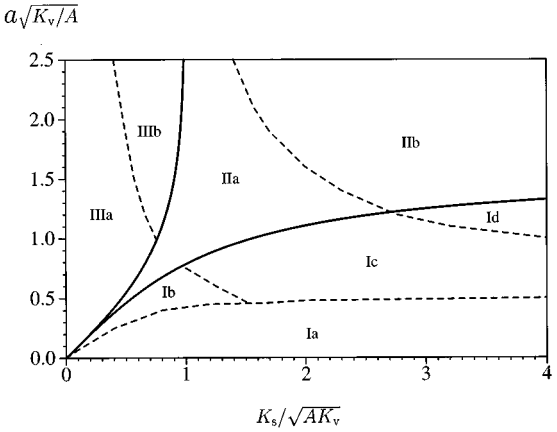

FIG. 2. Phase diagram for the dominant process of magnetization reversal in magnetic films in perpendicular fields. See text for explanation.

phenomenological argument, although both reversals are actually sharp jumps of magnetization between two uniform configurations.

In the Ib phase, almost perfect coherent rotation of magnetization begins as the field increases up to the nucleation field $H_{\perp n}$. The rotation proceeds as the field increases further. A sharp jump to UUC occurs as the field reaches $H_{\perp c}$. In the Ic phase, nucleation of the in-plane magnetization component occurs at the central part of film as the field increases to $H_{\perp n}$. Incoherent rotation of magnetization takes place as the field is increased further, because the surface magnetization is pinned by the surface anisotropy energy. Then a jump to UUC occurs as the field reaches $H_{\perp c}$.

In the Id phase, as the external field increases, nucleation of in-plane magnetization occurs first, and then the magnetization rotates incoherently toward the direction of the field. As the field increases further, nucleation of the upward magnetization component occurs at the central part of film, and the walls separating the regions with opposite normal magnetization components are pushed toward the film surfaces. Finally, the system jumps to UUC as the field increases to $H_{\perp c}$. The process of magnetization reversal in a system with $a\sqrt{K_v/A}=1.25$ and $K_s/\sqrt{AK_v}=4$ is displayed in Fig. 3.

In the IIa and IIb phases, the system behaves similarly as in the Ic and Id phases, respectively, except that $H_{\perp n}$ is negative and the jump of the system at $H_{c\perp}$ is to a nonuniform configuration with an upward normal component. As the field increases further, incoherent rotation of magnetization proceeds gradually, and the system saturates gradually to the UUC at a saturation field $H_{\perp s}$.

In the IIIa phase, the whole system rotates almost coherently toward the direction of the field as soon as the field is applied and the system saturates gradually to UUC at $H_{\perp s}$. In the IIIb phase, as the field is switched on, nucleation of upward magnetization components occurs at the surface, and incoherent rotation proceeds when the magnetization at the central part of film is pinned by the shape anisotropy energy. Incoherent rotation of magnetization proceeds gradually, and the system saturates to UUC at $H_{\perp s}$.

Thus, such processes as nucleations, coherent and incoherent rotations, domain-wall motion, and sharp jumps in the direction of magnetization are observed in the magnetization

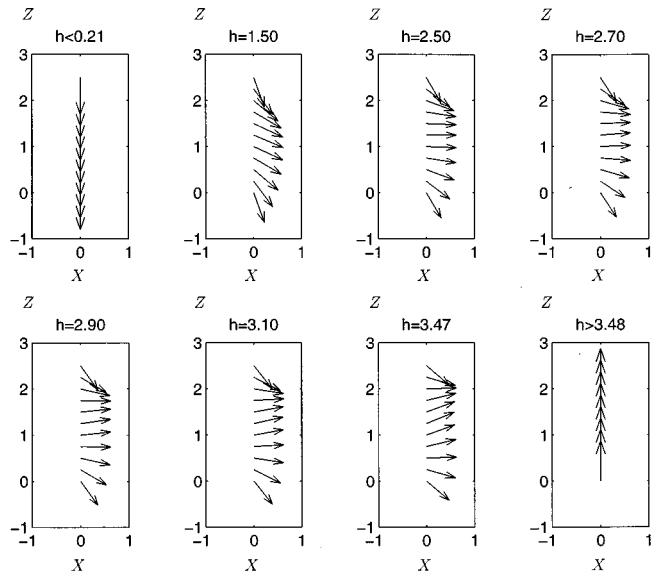

FIG. 3. Magnetization reversal process in the film of $a\sqrt{K_v/A}=1.25$ and $K_s/\sqrt{AK_v}=4.0$ in perpendicular fields. Nucleation of nonuniform configuration takes places at $h\equiv M_sH_\perp/K_v\simeq 0.21$. Nucleation of an upward magnetization component occurs in the central part of the film at a field of $h\simeq 2.6$.

reversal of ultrathin magnetic film by a perpendicular field. Which process is dominant for a given film depends on the relative strengths of the anisotropies and exchange stiffness, and on the film thickness, as described above and summarized in Fig. 2.

Hysteresis loops for an averaged normal magnetization component in perpendicular fields are plotted in Fig. 4 for thin magnetic films with $K_s/\sqrt{AK_v}=0.5$. As the film thickness increases, the shape of the hysteresis loop changes gradually from rectangular, at $a\sqrt{K_v/A}=0.4$, to S-shaped, at $a\sqrt{K_v/A}=0.5$, and finally shrinks to a single curve, at $a\sqrt{K_v/A}=1$. This change in shape of the hysteresis loop

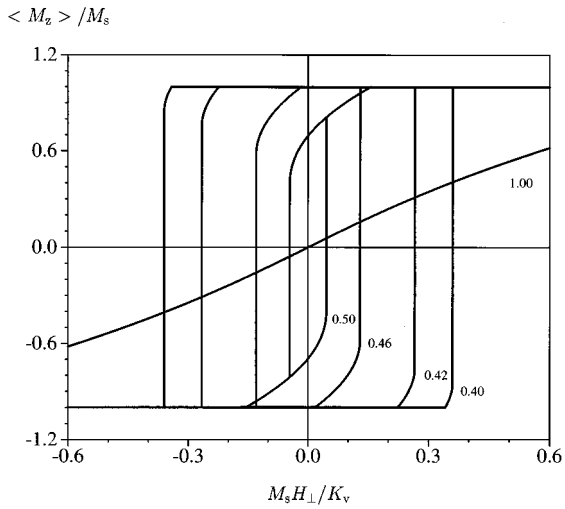

FIG. 4. Hysteresis loops of $\langle\cos\varphi\rangle$, the average normal component of magnetization normalized by the saturation magnetization, for films of thicknesses $a\sqrt{K_v/A}=0.4$, 0.42, 0.46, 0.5, and 1 in perpendicular fields. The surface anisotropy is $K_s/\sqrt{AK_v}=0.5$.

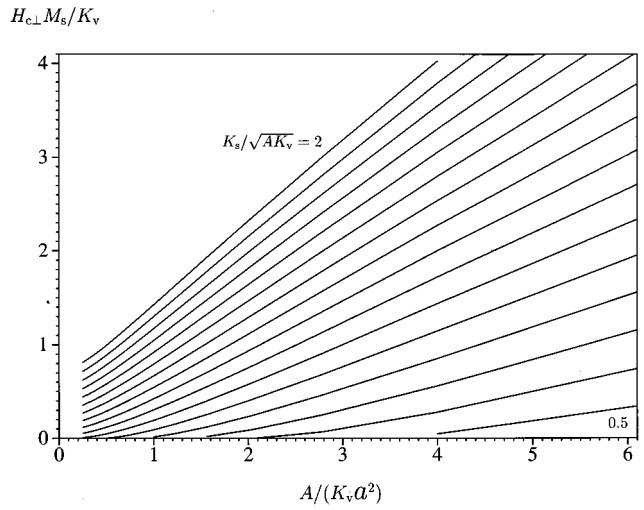

FIG. 5. Thickness dependence of coercivity of ultrathin films to perpendicular fields. Solid lines are for fixed values of surface anisotropy $K_s/\sqrt{AK_v}=0.5$ through 2. The difference between the surface anisotropies for neighboring lines is 0.1.

reflects the fact that the spin-reorientation transition occurs as the thickness increases in zero field and is consistent with experimental observations.

The coercivity of ultrathin magnetic films is estimated numerically by the present model. According to the discussion on the form of the equation of the magnetization configuration in the preceding section and the experimental observations on the thickness dependence of coercivity, we plot the evaluated coercive force as a function of the square of the reciprocal of the film thickness in Fig. 5. The linearity demonstrates that the coercivity decays in proportion to the square of the reciprocal thickness, as has been observed in experiments.[8,14,15] We have calculated the coercive force for $K_s/\sqrt{AK_v}$ down to 0.1, and have found similar thickness dependences as shown in Fig. 5. The data for the small surface anisotropies are omitted from Fig. 5 because the associated values of the square of the reciprocal thickness are too large.

The origin of this thickness dependence of coercivity is as follows: The film thickness appears in Eqs. (2), (3), (5), and (6) only in the form $a\sqrt{K_v/A}\sqrt{\cos\varphi_a+h_\perp/2}$. At external fields close to the coercive force, a relation $\cos\varphi_a\sim h_\perp+c$, where c is a constant, is established for various thicknesses, as shown in Fig. 4. Therefore, the thickness is scaled by the strength of field as $a\sqrt{K_v/A}\sqrt{h_\perp+2c/3}$ at fields near to the coercivity. Since the other contributions from the strength of external field in Eqs. (2), (3), (5), and (6) cancel each other, the scaling between the thickness and the external field results in the dependence of the coercivity on the square of the reciprocal thickness. Therefore, we obtain the following expression for the coercivity:

$$H_{\perp c}=B\,\frac{K_v}{M_s}+C\,\frac{A}{M_s a^2}. \tag{9}$$

Figure 5 also shows that the coercive force increases linearly with the surface anisotropy. We thus have B and C proportional to the surface anisotropy K_s. A similar expression to Eq. (9) has been derived for nucleation field with $B=2$ and $C=2\pi^2$.[24]

IV. MAGNETIZATION REVERSALS IN IN-PLANE FIELDS

The approach in the preceding section can be applied to external fields of any orientation. As an important case, we discuss the case of in-plane field. For convenience of calculation, the energy functional is expressed using the angle ψ defined in Fig. 1:

$$\gamma=\int_0^a\left[A\left(\frac{d\psi}{dz}\right)^2-K_v\cos^2\psi+H_\parallel M_s\cos\psi\right]dz+K_s\cos^2\psi(0). \tag{10}$$

The orientation of magnetization at the center of the film is determined by

$$\frac{K_s}{\sqrt{AK_v}}=\frac{\mathrm{cn}^2[x_3,k_3]+\tan^2(\psi_a/2)}{\mathrm{cn}^2[x_3,k_3]-\tan^2(\psi_a/2)}\sqrt{\cos\psi_a-h_\parallel/2}\times\frac{\mathrm{sn}[x_3,k_3]\mathrm{dn}[x_3,k_3]}{\mathrm{cn}[x_3,k_3]}, \tag{11}$$

where

$$x_3=a\sqrt{K_v/A}\sqrt{\cos\psi_a-h_\parallel/2},$$

$$k_3=\cos\left(\frac{\psi_a}{2}\right)\sqrt{(1+\cos\psi_a-h_\parallel)/(2\cos\psi_a-h_\parallel)},$$

$$h_\parallel\equiv H_\parallel M_s/K_v, \tag{12}$$

if $-1+\cos\psi_a-h_\parallel>0$. The total configuration is

$$\tan\left(\frac{\psi(z)}{2}\right)=\frac{\tan(\psi_a/2)}{\mathrm{cn}[(a-z)\sqrt{K_v/A}\sqrt{\cos\psi_a-h_\parallel/2},k_3]}. \tag{13}$$

For $-1+\cos\psi_a-h_\parallel<0$,

$$\frac{K_s}{\sqrt{AK_v}}=\frac{\mathrm{dn}^2[x_4,k_4]+\tan^2(\psi_a/2)}{\mathrm{dn}^2[x_4,k_4]-\tan^2(\psi_a/2)}\times\frac{2\cos\psi_a-h_\parallel}{\sqrt{(1+\cos\psi_a)(1+\cos\psi_a-h_\parallel)}}\times\frac{\mathrm{sn}[x_4,k_4]\mathrm{cn}[x_4,k_4]}{\mathrm{dn}[x_4,k_4]}, \tag{14}$$

where

$$x_4=a\sqrt{K_v/A}\sqrt{(1+\cos\psi_a)(1+\cos\psi_a-h_\parallel)}/2,$$

$$k_4=\sqrt{(4\cos\psi_a-2h_\parallel)/[(1+\cos\psi_a)(1+\cos\psi_a-h_\parallel)]}, \tag{15}$$

and the total configuration is

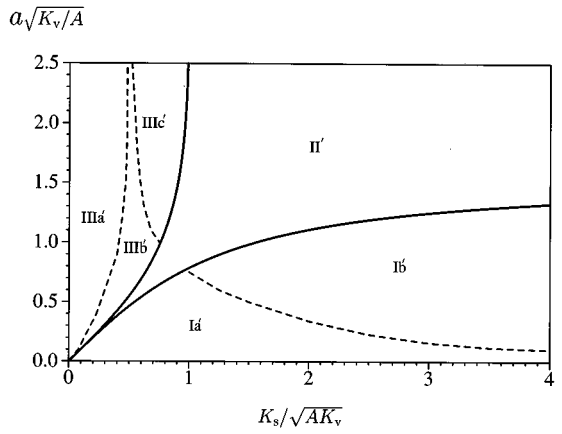

FIG. 6. Phase diagram for the dominant process of magnetization reversal in magnetic films in in-plane fields. See text for explanation.

$$\tan\left(\frac{\psi(z)}{2}\right) = \frac{\tan(\psi_a/2)}{\mathrm{dn}[(a-z)\sqrt{K_v/A}\sqrt{(1+\cos\psi_a)(1+\cos\psi_a-h_\parallel)}/2,k_4]}. \tag{16}$$

By putting $\psi_a=0$ in Eqs. (14) and (15), we can derive the equation for nucleation field of nonuniform magnetization configuration[10]

$$\frac{K_s}{\sqrt{AK_v}} = \sqrt{1-h_{\parallel n}}\,\tanh(a\sqrt{K_v/A}\sqrt{1-h_{\parallel n}}). \tag{17}$$

A positive nucleation field determined by Eq. (17) can be shown analytically to be smaller than $2(K_v-K_s/a)/M_s$, the coercive force obtained from phenomenological arguments, by noting that $x>\tanh x$ for $x>0$. For a system with a negative nucleation field, there is a saturation field with the same absolute value of the nucleation field.

The phase diagram for response of the system to in-plane external fields is presented in Fig. 6. In the Ia′ phase, the magnetization of the system rotates coherently from the DUC to the direction of field as soon as the field is applied, and saturates gradually to the leftward uniform configuration (LUC) at the saturation field $H_{\parallel s}$. In the Ib′ phase, nucleation of in-plane magnetization components occurs in the central part of the film as soon as the field is applied. As the field increases, incoherent rotation of magnetization occurs as the magnetization at the surface is pinned by the surface anisotropy energy. The system saturates gradually to LUC at $H_{\parallel s}$.

In the IIIa′ phase, the system remains at an initial rightward uniform configuration (RUC) until the field reaches the coercivity $H_{\parallel c}$, at which the system jumps abruptly to LUC. In the IIIb′ phase, magnetization begins to rotate coherently toward the direction of the field after the field strength becomes larger than the nucleation field $H_{\parallel n}$. The rotation proceeds as the field increases further, and finally the system jumps sharply to LUC at $H_{\parallel c}$. In the IIIc′ phase, nucleation of the perpendicular magnetization components occurs at the surface after the field reaches $H_{\parallel n}$, and then incoherent rotation of magnetization toward the direction of the field proceeds as the field increases. The system jumps to LUC at $H_{\parallel c}$.

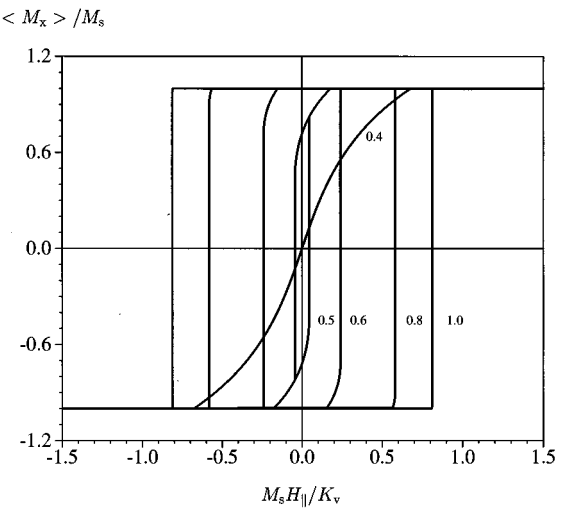

FIG. 7. Hysteresis loops of $\langle\cos\psi\rangle$, the average in-plane component of magnetization normalized by the saturation magnetization, for films of thicknesses $a\sqrt{K_v/A}=0.4$, 0.5, 0.6, 0.8, and 1 in in-plane fields. The surface anisotropy is $K_s/\sqrt{AK_v}=0.5$.

In the II′ phase, the system behaves similarly as in the IIIc′ phase, except that the nucleation field is negative and that at $H_{\parallel c}$ the system jumps to a leftward nonuniform configuration. As the field increases further, incoherent rotation of magnetization proceeds and the system saturates gradually to LUC at $H_{\parallel s}$.

As was the case for perpendicular fields, nucleations, coherent and incoherent rotations and abrupt jumps in the magnetization reversal of ultrathin magnetic films are again observed for in-plane magnetic fields. In this case, no nucleation of opposite in-plane magnetization component to the initial configuration occurs before the sharp jump of the direction of magnetization at $H_{\parallel c}$. Thus, domain-wall motion in the direction of the film normal does not contribute to magnetization reversals of thin magnetic films in in-plane fields.

Hysteresis loops for an averaged in-plane magnetization component in in-plane fields are displayed in Fig. 7 for thin magnetic films with $K_s/\sqrt{AK_v}=0.5$. As the film thickness decreases, the shape of the hysteresis loop changes gradually from rectangular, at $a\sqrt{K_v/A}=1$, to S-shaped, at $a\sqrt{K_v/A}=0.5$, and finally shrinks to a single curve, at $a\sqrt{K_v/A}=0.4$. This variation of the shape of the hysteresis loop again corresponds to the spin-reorientation transition occurring as the thickness varies in zero field.

We evaluated the coercivity of thin films to in-plane external fields. The values of coercive force are displayed as a function of the reciprocal of the film thickness in Fig. 8 where the strength of surface anisotropy $K_s/\sqrt{AK_v}$ is a parameter and is taken from 0.1 to 2. The coercivity increases linearly with the reciprocal of the thickness for small surface anisotropy. This behavior can be explained as follows: In films with small surface anisotropies the direction of magnetization at the center of the film remains almost in-plane, that is $\psi_a\simeq 0$, even in the vicinity of the coercivity. In these films,

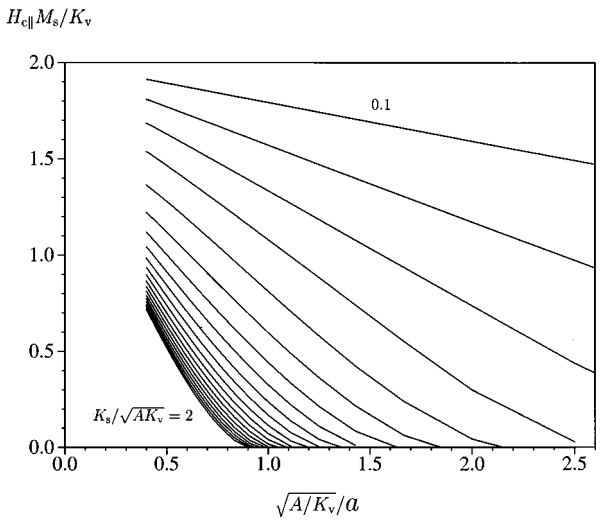

FIG. 8. Thickness dependence of coercivity of ultrathin films to in-plane fields. Solid lines are for fixed values of surface anisotropy $K_s/\sqrt{AK_v}=0.1$ through 2. The difference between the surface anisotropies for neighboring lines is 0.1.

Eq. (17) gives a good approximation of the coercive force. Since surface anisotropy is small, one has from Eq. (17)

$$\frac{K_s}{\sqrt{AK_v}}=(1-h_{\|c})a\sqrt{K_v/A}. \tag{18}$$

For large surface anisotropy, the coercive force shows a more complex thickness dependence. However, as seen in Fig. 8, the linear reciprocal-thickness law for the coercivity gives a fairly good description for all values of surface anisotropy.

V. DISCUSSIONS AND SUMMARY

Since direct experimental observation of microscopic magnetization processes occurring on the length scale of 1 nm is not yet available, theoretical analyses and predictions are useful for the development of imaging techniques and the improvement of the performance of high-density memory storage devices. In this work, we studied the magnetic reversal processes in ultrathin magnetic films using a continuum micromagnetic model.

An approximation on the magnetization configuration in in-plane directions is adopted in the present work. Although the dipolar interactions favor a structure of stripes of antiparallel oriented magnetic domains next to each other across an ultrathin magnetic film, the domains are typically of the order of micrometers in size.[9] These are much larger than the domain-wall thicknesses of the order of tens of nanometers and film thicknesses of the order of 1 nm. Therefore, the magnetic structure can be considered as virtually uniform and of infinite extension in the in-plane directions. In literature, on the other hand, the uniformity of magnetization in the film-normal direction is assumed and the effect of surface anisotropy is merely included in a total effective anisotropy. Therefore, the two approaches are complimentary to each other.

Our approach shows analytically that, for a magnetic film with normal/in-plane uniform configuration in zero field, change in magnetization configuration is caused by a strength of perpendicular/in-plane field smaller than the value predicted by phenomenological arguments. The manner of change in the magnetization configuration of an ultrathin film can proceed by nucleation of structure nonuniform in the direction of the film normal, or by coherent rotation of magnetization toward the direction of the field, or by abrupt jumps to reversed uniform configuration. Incoherent rotation of magnetization and domain-wall motion also occur during reversals. The dominant process of magnetization reversal in a thin magnetic film is determined by the two scaling variables $a\sqrt{K_v/A}$ and $K_s/\sqrt{AK_v}$ as shown in two phase diagrams for perpendicular and in-plane fields.

We derived equations for the magnetization configurations of ultrathin films under external fields and obtained both analytic and numerical evidence of the dependence of the coercivity on the square of the reciprocal thickness in perpendicular fields. Our theoretically derived thickness dependence of the coercivity coincides very well with experimental observations.

We also studied the magnetization reversal in thin magnetic films by an in-plane field. Particularly, the coercive force increases linearly with the reciprocal thickness. Discrepancies between the predicted and measured values of coercivity remain an important problem.

ACKNOWLEDGMENTS

The author thanks R. B. Goldfarb and J. O. Oti for fruitful discussions and suggestions. He gratefully acknowledges the hospitality extended to him during his tenure at NIST-Boulder.

*Present address: National Research Institute for Metals, 1-2-1 Sengen, Tsukuba 305, Japan.

[1] M. N. Baibich, J. M. Broto, A. Fert, F. Nguyen van Dau, F. Petroff, P. Etienne, G. Creuzet, A. Friederich, and J. Chazelas, Phys. Rev. Lett. **61**, 2472 (1988).

[2] J. Ferré, G. Pénissard, C. Marlière, D. Renard, P. Beanvillain, and J. P. Renard, Appl. Phys. Lett. **56**, 1588 (1990).

[3] E. C. Stoner and E. P. Wohlfarth, Trans. R. Soc. London Ser. A. **240**, 599 (1948).

[4] W. F. Brown, Jr., J. Appl. Phys. **30**, 625 (1959).

[5] A. Aharoni, Phys. Rev. **19**, 127 (1960).

[6] U. Gradmann, Appl. Phys. **3**, 161 (1974).

[7] B. Heinrich, K. B. Urquhart, A. S. Arrott, J. F. Cochran, K. Myrtle, and S. T. Purcell, Phys. Rev. Lett. **59**, 1756 (1987).

[8] C. Chappert and P. Bruno, J. Appl. Phys. **64**, 5736 (1988).

[9] R. Allenspach, M. Stampanoni, and A. Bischof, Phys. Rev. Lett. **65**, 3344 (1990).

[10] A. Thiaville and A. Fert, J. Magn. Magn. Mater. **113**, 161 (1992).

[11] H. Fritzsche, J. Kohlhepp, H. J. Elmers, and U. Gradmann, Phys. Rev. B **49**, 15 665 (1994).

[12] X. Hu and Y. Kawazoe, Phys. Rev. B **51**, 311 (1995).

[13] X. Hu, R.-B. Tao, and Y. Kawazoe, Phys. Rev. B **54**, 65 (1996).

[14] P. Bruno, J. Appl. Phys. **68**, 5759 (1990).

[15] C. Chappert, P. Beauvillain, P. Bruno, J. P. Chauyineau, M.

Galtier, K. Le Dang, C. Marlière, R. Mégy, D. Renard, J. P. Renard, J. Seiden, F. Trigui, P. Veillet, and E. Vélu, J. Magn. Magn. Mater. **93**, 319 (1991).
[16] T. Kingetsu, Jpn. Appl. Phys. **33**, L1406 (1994).
[17] J. Pommier, P. Meyer, G. Pénissard, J. Ferré, P. Bruno, and D. Renard, Phys. Rev. Lett. **65**, 2054 (1990).
[18] B. Heinrich, J. F. Cochran, A. S. Arrott, S. T. Purcell, K. B. Urquhart, S. R. Dutcher, and W. F. Egelhoff, Appl. Phys. A **49**, 473 (1989).
[19] J. P. Gay and R. Richter, Phys. Rev. Lett. **56**, 2728 (1986); J. Appl. Phys. **61**, 3362 (1987).
[20] N. Bardou, B. Bartenlian, C. Chappert, R. Mégy, P. Veillet, and J. P. Renard, J. Appl. Phys. **79**, 5848 (1996).
[21] L. Néel, J. Phys. Rad. **15**, 376 (1954).
[22] D. L. Mills, Phys. Rev. B **39**, 12 306 (1989); R. C. O'Handley and J. P. Woods, *ibid*. **42**, 6568 (1990); A. Aharoni, *ibid*. **47**, 8296 (1993).
[23] X. Hu and Y. Kawazoe, Phys. Rev. B **49**, 3294 (1994).
[24] H. Kronmüller and H. R. Hilzinger, J. Magn. Magn. Mater. **2**, 3 (1976).